Stress-induced changes in magnetite: insights from a numerical analysis of the Verwey transition

Helena Fuchs [1], Agnes Kontny[2] and Frank R. Schilling[1]

[1]*Institute of Applied Geosciences, Technical Petrophysics, Karlsruhe Institute of Technology, Adenauerring* 20*b,* 76131 *Karlsruhe, Germany. E-mail:*
helena.fuchs@kit.edu
[2]*Institute of Applied Geosciences, Structural Geology & Tectonics, Karlsruhe Institute of Technology, Adenauerring* 20*a,* 76131 *Karlsruhe, Germany*

SUMMARY
Magnetic susceptibility behaviour around the Verwey transition of magnetite ($\approx$125 K) is known to be sensitive to stress, composition and oxidation. From the isotropic point ($\approx$130 K) to room temperature, decreasing magnetic susceptibility indicates an increase in magnetocrystalline anisotropy. In this study, we present a model which numerically analyses low-temperature magnetic susceptibility curves (80–280 K) of an experimentally shocked (up to 30 GPa) and later heated (973 K) magnetite ore. To quantify variations of the transition shape caused by both shock and heating, the model statistically describes local variations in the Verwey transition temperature within bulk magnetite. For the description, Voigt profiles are used, which indicate variations between a Gaussian and a Lorentzian character. These changes are generally interpreted as variations in the degree of correlation between observed events, that is between local transition temperatures in the model. Shock pressures exceeding the Hugoniot elastic limit of magnetite ($\geq$5 GPa) cause an increase in transition width and Verwey transition temperature, which is partially recovered by heat treatment. Above the Verwey transition temperature, susceptibility variations related to the magnetocrystalline anisotropy are described with an exponential approach. The room temperature magnetic susceptibility relative to the maximum near the isotropic point is reduced after shock, which is related to grain size reduction. Since significant oxidation and cation substitution can be excluded for the studied samples, variations are only attributed to changes in elastic strain associated with shock-induced deformation and annealing due to heat treatment. The shocked magnetite shows a high correlation between local transition temperatures which is reduced by heat treatment. The model allows a quantitative description of low-temperature magnetic susceptibility curves of experimentally shocked and subsequently heat-treated polycrystalline magnetite around the Verwey transition temperature. The curves are accurately reproduced within the experimental uncertainties. Further applications for analysing magnetite-bearing rocks seem possible if model parameters, such as for oxidation are included into the model.

Key words: Defects; Numerical modelling; Magnetic properties; Phase transitions.

1 INTRODUCTION

Magnetite is an accessory mineral in many rock types. Due to its strong ferrimagnetic behaviour it is an important mineral for rock and palaeomagnetic analyses. Magnetite undergoes a structural phase transition from a low-temperature monoclinic phase to a cubic phase at about 125 K, called the Verwey transition (Verwey 1939; Walz 2002). The phase transition causes characteristic changes in magnetic (see e.g. Muxworthy & McClelland 2000) as well as in thermodynamic and electrical properties (e.g. Kąkol *et al.* 1992; Kozłowski *et al.* 1996a).

Numerous studies have considered the effect of external stress on the Verwey transition. Some studies report an approximately linear decrease of the Verwey transition temperature T_V with variable slope under quasi-hydrostatic pressure p (Samara 1968; Kakudate *et al.* 1979; Tamura 1990; Ramasesha *et al.* 1994; Sato *et al.* 2012) while a discontinuous change of T_V was observed, for example by Rozenberg *et al.* (1996) from 107.5 to 100 K at about 6 GPa. More recent studies indicate that T_V decreases linearly towards 0 K at about 20 GPa in stoichiometric magnetite under quasi-hydrostatic pressure (Gasparov *et al.* 2005; Muramatsu *et al.* 2016). These discrepancies might be related to non-stoichiometry

(Gasparov *et al.* 2012). Under directional strain, positive slopes of dT_V/dp were observed experimentally (Nagasawa *et al.* 2007), and for non-hydrostatic pressure both positive and negative slopes were determined theoretically depending on the stress orientation (Coe *et al.* 2012).

The way static external pressure affects the magnetic behaviour on a microscopic scale differs from the mechanisms in decompressed magnetite. Static pressure affects the electronic structure whereas in a post-shock state changes in the magnetic behaviour are mainly controlled by the formation of defects (Biało *et al.* 2019). Carporzen & Gilder (2010) found a positive slope of dT_V/dp in magnetite decompressed from hydrostatic pressure.

Internal stresses must be considered for the post-shock state as they can be related to dislocations or misfits at phase boundaries in magnetite. The influence of microstress on domain wall controlled coercivity was documented by Moskowitz (1993) by a 1-D micromagnetic model for grains with high and low defect densities (e.g. recrystallized magnetite). Lindquist *et al.* (2015) showed that stress-induced dislocations cause pinning of magnetic domain walls in multidomain magnetite and an increase of microcoercivity in dislocation-rich areas. Upon cooling through T_V, internal stress fields impede monoclinic twinning and the direction of stress affects the orientation of monoclinic twins (Williams *et al.* 1953; Calhoun 1954; Coe *et al.* 2012; Lindquist *et al.* 2019). Coe *et al.* (2012) suggested that a complex internal stress field caused by dislocations and other defects results in broadened Verwey transitions and local variations of T_V.

At T_V, a change in electron order occurs, which is related to a slight lattice distortion (e.g. Senn *et al.* 2012), and therefore the transition itself causes spontaneous strain (Coe *et al.* 2012). The strain dependence of T_V as function of small cation substitution has been investigated by Biało *et al.* (2019). These authors observed that pressure cycling to $\approx$5 GPa has an impact on T_V and coercivity by pinning the magnetic domains on interstitial cations and structural lattice distortions. Deviations from stoichiometry, either by cation vacancies (Aragón *et al.* 1985) or by substitution of iron by various metal cations (e.g. Kozłowski *et al.* 1996b; Brabers *et al.* 1998; Wiecheć *et al.* 2005) shift T_V to lower temperatures. Non-stoichiometry also broadens the transition (e.g. Honig 1995). Jackson & Moskowitz (2021) observed a bimodal distribution of T_V between about 100 and 110 K in a large set of magnetite samples of various natural and synthetic origins, which is explained by variations in non-stoichiometric magnetite (Honig 1995).

At about 130 K, which is slightly above T_V, magnetite passes through a magnetically isotropic point, where the first magnetocrystalline anisotropy constant K_1 changes sign and the magnetic easy axes reorient within the cubic spinel lattice. Typically, the effect of the isotropic point on the magnetic property changes with temperature is minor compared to the effect of T_V, but the commonly observed decrease in magnetic susceptibility χ from the isotropic point to room temperature is expected to be related to an increase in magnetocrystalline anisotropy over that range (Bickford *et al.* 1957; Muxworthy & McClelland 2000). According to Aragón *et al.* (1985), a more pronounced curvature in magnetic susceptibility above the isotropic point is related to the polycrystalline nature of the material, and Muxworthy & McClelland (2000) emphasize that a stronger increase of the magnetocrystalline anisotropy above the isotropic point is related to an increasing contribution of the second cubic anisotropy constant K_2, which is nearly insignificant above room temperature (Bickford *et al.* 1957; Syono 1965).

Because of its sensitivity to changes in stress state and stoichiometry, the Verwey transition morphology can serve as a possible indicator of shock pressure in impact-related rocks. Two Verwey temperatures were identified in basement rocks of the Vredefort impact crater and attributed to a pre-impact magnetite population and a population with impact-related formation showing significantly reduced T_V (Carporzen *et al.* 2006). A lower T_V attributed to oxidation probably related to post-shock alteration was found in impacted crystalline basement rocks from the Chesapeake Bay impact structure (Mang & Kontny 2013) and in volcanic rocks from the El'gygytgyn impact structure (Kontny & Grothaus 2017). Reznik *et al.* (2016) identified an increase of T_V by around 4 K and a broadening of the transition in experimentally shocked magnetite (Fig. 1a). Kontny *et al.* (2018) studied the same samples after a heat treatment up to 973 K and observed a recovery of both T_V and the transition width related to annealing of shock-induced defects and dislocations by recrystallization (Fig. 1b). The results of these authors indicate that the χ-T behaviour of shocked and annealed magnetite is also sensitive to the decrease of χ between the isotropic point and room temperature.

A more detailed description of magnetic susceptibility in the region of the Verwey transition may be useful to better distinguish between these effects. The determination of T_V and the transition width often considers $d\chi/dT$, focusing on the sharp susceptibility increase near T_V (e.g. Carporzen & Gilder 2010; Reznik *et al.* 2016; Kontny *et al.* 2018). The model introduced in this study uses the experimental temperature range from about 80 to 280 K for the determination of model parameters. To test the approach and to quantify and visualize the effect of shock deformation on the Verwey transition, the model is applied to the χ-T curves measured by Reznik *et al.* (2016) and Kontny *et al.* (2018) on shocked and subsequently heat-treated magnetite ore (Fig. 1). Furthermore, a χ-T curve of the same ore shocked at 3 GPa using the same experimental setup and heat treatment is evaluated.

2 VERWEY TRANSITION MODEL

2.1 Model formulation for an idealized small magnetite volume

The presented model approach is tested on χ-T curves of a well-characterized magnetite ore exhibiting stress-induced features in magnetite without cation substitution or oxidation (Reznik *et al.* 2016; Kontny *et al.* 2018). For consideration of other effects like cation substitution or oxidation, adjustments to the model will be necessary. Contributions to the bulk susceptibility by minerals other than magnetite (quartz, amphibole, chlorite, biotite and pyrite) can be neglected, either because of their low susceptibility compared to magnetite (e.g. Hunt *et al.* 1995) or because of their low content in the studied samples. In the examined temperature range, background susceptibility shows negligible thermal variations compared to those due to magnetite. For a better comparability of the curve shape between the initial, shocked and reheated samples, the χ-T curves are normalized to values between zero and one.

The model assumes that a small magnetite volume, which can be considered homogeneous with regard to factors that influence the transition temperature, has a certain transition temperature T_{Vd} at which it transforms instantaneously. This assumption corresponds to a first order phase transition. A change to a second order transition is related to non-stoichiometry (e.g. Aragón *et al.* 1985) and is observed at static pressures above 6 GPa (Rozenberg *et al.* 1996).
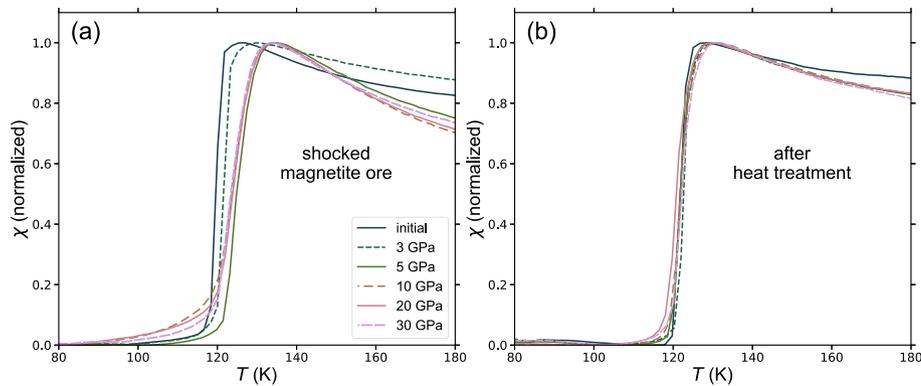
Figure 1. (a) Normalized χ-T curves of the initial and shocked magnetite ore samples (Reznik *et al.* 2016) and of a sample of the same magnetite ore shocked at 3 GPa. (b) χ-T curves of the same samples after heat treatment to 973 K (Kontny *et al.* 2018).

The susceptibility was measured in the decompressed post-shock state and therefore it is not likely that the magnetite underwent a second order phase transition during the susceptibility measurement. Parameters related to such a model volume fraction are denoted by subscript d to distinguish them from bulk magnetite properties. For the magnetite analysed in this study, shock-related deformation and dislocations can be considered as the main factors affecting the size of the volume. The model volume idealizes the microscopic processes involved in the Verwey transition and cannot be directly related to, for example a magnetic domain, although it is assumed to be of a similar scale. Below T_{Vd}, the susceptibility χ_d of the volume fraction is assumed to be constant and equal to zero due to normalization:

$$\chi_d(T) = 0 \text{ for } T < T_{\mathrm{Vd}}. \tag{1}$$

Especially the magnetite ore shocked at 10 GPa and above shows a significant susceptibility increase already at the lower experimental limit ($\approx$80 K). Thermal susceptibility variations below the Verwey transition are attributed to changes of easy magnetic axes orientation in twins of the monoclinic phase, which can be induced by an external magnetic field (e.g. Kosterov 2003; Kosterov & Fabian 2008). The frequency of orientation changes increases with temperature due to the higher thermal energy. For the analysed χ-T curves, a clear numerical distinction between these low-temperature processes and the Verwey transition is not possible. At temperatures above of the Verwey transition, the magnetic susceptibility of magnetite exhibits a maximum related to the isotropic point at about 130 K that is especially in single crystals, often exhibited as a distinct peak. The analysed magnetite does not show a distinct peak close to 130 K but a rather broad susceptibility maximum. Therefore, the numerical approximation of these χ-T curves does not require a specific consideration of the isotropic point.

Especially for magnetite shocked at 5 GPa and above, the susceptibility at room temperature relative to the isotropic point is significantly lower and partially recovers in form of a relative increase of susceptibility after heating. To describe these changes, χ_d at temperatures above T_{Vd} is assumed to be the sum of a temperature-independent susceptibility contribution χ_{0d} and a temperature-dependent part $\chi_{1d}(T)$:

$$\chi_d(T) = \chi_{0d} + \chi_{1d}(T) \text{ for } T \geq T_{\mathrm{Vd}}. \tag{2}$$

Parameters affecting the constant part of χ are denoted with subscript 0 and parameters of the temperature-dependent part with 1. In the model, the decrease of the magnetic susceptibility above T_{Vd} is not regarded as directly related to the Verwey transition. The
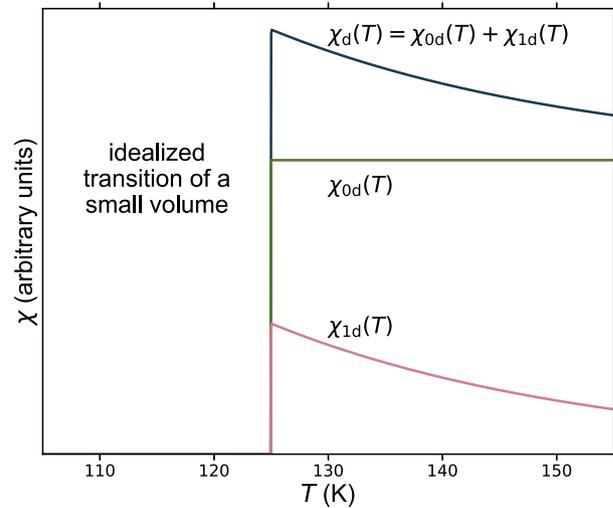
Figure 2. Modelled χ-T curve of a homogeneous magnetite volume fraction with $T_{\mathbf{Vd}} = 125\,\mathbf{K}$ (eq. 14). These curves represent an idealized Verwey transition with zero width. Below $T_{\mathbf{Vd}}$, the susceptibility of the volume fraction $\chi_{\mathbf{d}}(T)$ is zero and above $T_{\mathbf{Vd}}$, $\chi_{\mathbf{d}}(T)$ is modelled with a sum of a constant component $\chi_{0\mathbf{d}}$ and of an exponentially decreasing component $\chi_{1\mathbf{d}}(T)$. Model parameters: $r_{1\mathbf{d}} = 0.035$; $c_{1\mathbf{d}} = 0.3$.

ratio of $\chi_{1d}(T)$ to $\chi_d(T)$ at T_{Vd} is used as model parameter c_{1d} to describe the temperature-dependent susceptibility above T_{Vd}:

$$c_{1d} = \frac{\chi_{1d}(T_{\mathrm{Vd}})}{\chi_d(T_{\mathrm{Vd}})}. \tag{3}$$

The susceptibility decrease between the isotropic point and room temperature is related to the increase of the magnetocrystalline anisotropy in multidomain magnetite grains (Muxworthy 1999). The model uses an exponential approach for a basic numerical description of the observed decrease above the transition:

$$\chi_{1d}(T) = \chi_{1d}(T_{\mathrm{Vd}})(1 - r_{1d})^{(T-T_{\mathrm{Vd}})/a}. \tag{4}$$

The dimensional number a is required for an exponent without dimension of a temperature. Temperatures in this study are given in Kelvin ($a = 1\,\mathrm{K}$). The rate of the exponential susceptibility decrease is described by the parameter r_{1d}. An example of a magnetite volume with $T_{\mathrm{Vd}} = 125\,\mathrm{K}$ is shown in Fig. 2.

2.2 Model Verwey transition temperature distribution in bulk magnetite

The model uses statistical distributions of T_{Vd} over the magnetite volume to describe the effect of, for example local stress states on the local transition temperature (Fig. 3a). The model uses symmetric distributions to reflect an overall balanced stress state in the sample during the χ-T measurements. A Voigt profile is the convolution of a Gaussian and a Lorentzian curve and these curve shapes represent boundary conditions. A Gaussian distribution results from uncorrelated events whereas a Lorentzian distribution indicates a correlation between events (e.g. Succi & Coveney 2019). In terms of a physical interpretation, a Gaussian distribution indicates that for all volume fractions, T_{Vd} is independent from T_{Vd} of other volume fractions whereas a Lorentzian distribution results from a correlation of T_{Vd} between volume fractions.

In various spectroscopic methods, Gaussian and Lorentzian distributions are used to characterize variations in line shape that may be related to dislocations and point defects (e.g. Stoneham 1969; Major *et al.* 2020). Voigt distributions of lattice strain are used to describe diffraction patterns (e.g. Csikor & Groma 2004). Shapes of X-ray diffraction (XRD) line profiles are related to the distribution of internal lattice strain. The convolution integral of a Voigt profile can be expressed through the real part of the Faddeeva function $w(z)$. The Faddeeva function is a scaled complex complementary error function:

$$w(z) = e^{-z^2} \, erfc(-iz). \tag{5}$$

For computation of the Faddeeva function, the Python module scipy.special.wofz is used. The source code of the package uses a combination of different algorithms (see Johnson 2012). To calculate the bulk susceptibility from the idealized χ-T curves for specific local transition temperatures, they are scaled by a dimensionless value $v_{Td}(T)$, corresponding to the value of the distribution of T_{Vd}. Based on the Faddeeva function, the expression for $v_{Td}(T)$ that is used in the Verwey transition model is

$$v_{Td}(T) = \frac{Re[w(z)]}{\sigma_V \sqrt{2\pi}}, \tag{6}$$

where z is:

$$z = \frac{T_{Vd} - \bar{T}_V + i\gamma_V}{\sigma_V \sqrt{2}}. \tag{7}$$

The centre $\bar{T}_V$ of the distribution is the model temperature at which the largest volume fraction experiences the susceptibility increase. In this study, $\bar{T}_V$ is determined by the fitting process. The parameter $\bar{T}_V$ is close to T_V, determined from the maximum of $d\chi/dT$. In the following, the model parameter is referred to as $\bar{T}_V$, while T_V is used for other evaluation approaches and the Verwey temperature in general.

The shape of the Voigt profile is defined by the ratio of the scale parameters σ_V and γ_V of the convolved Gaussian and Lorentzian distributions, which are determined by fitting. For $\gamma_V/\sigma_V \gg 1$ the profile approximates a Lorentzian distribution, whereas for $\gamma_V/\sigma_V \ll 1$ it approximates a Gaussian distribution. For $\sigma_V = 0$ and $\gamma_V = 0$ the Voigt profile is a Lorentzian and Gaussian distribution, respectively (e.g. Armstrong 1967). A Gaussian distribution leads to a more pronounced peak at the transition, whereas a Lorentzian distribution leads to a significant increase in susceptibility at low temperatures and a smoother transition.

The bulk χ-T curve is the sum of all contributions to χ, since the bulk susceptibility is the sum of the magnetic moments of all volume fractions of magnetite. The summation leads to a broadening and a smoothing of the model curve, similar to the experimental curve shape (Fig. 3b). In the temperature range where a significant model volume passes through the Verwey transition, the resulting bulk curve is affected by both the susceptibility increase and the decrease above T_{Vd}. This range can exceed the sharp increase in susceptibility (see Figs 3a and b). At higher temperatures, the model curve is not significantly affected by the Verwey transition, but is controlled by the susceptibility decrease (c_{1d}, r_{1d}).

2.3 Effect of model parameters

To illustrate the effect of c_{1d}, σ_V and r_{1d} on a bulk χ-T curve based on a Gaussian distribution of T_{Vd}, individual parameters were varied while the other parameters were set to fixed values (see Fig. 4). Variations in $\bar{T}_V$ cause a temperature shift of the χ-T curve without affecting the shape of the curve. The effect of variations in the relative susceptibility decrease c_{1d} is shown in Fig. 4(a). Without a temperature independent component ($c_{1d} = 1$), susceptibility at high temperatures approaches zero. For $c_{1d} = 0$, the susceptibility does not decrease above the transition. An increase in σ_V or γ_V results in a broadening of the transition (Fig. 4b). When the rate of the exponential decrease r_{1d} is large, the susceptibility decreases rapidly above the Verwey transition (Fig. 4c). For the evaluation, c_{1d} and r_{1d} were constrained to a common variable value for all volume fractions. Curve scaling is used to compensate for varying peak heights (Fig. 4) The fitting was done using Python 3.9.13.

2.4 Experimental

Metamorphosed banded quartz-magnetite ore from the Sydvaranger mine (Norway) was used for the shock experiments (Reznik *et al.* 2016; Kontny *et al.* 2018). The ore contains about 80 weight per cent magnetite, 18 weight per cent quartz and 2 weight per cent accessory minerals including amphibole, chlorite, biotite and pyrite in bright quartz-rich and dark magnetite-rich bands (Reznik *et al.* 2016). The magnetite bands consist of polycrystalline and elongated grains. Scanning electron microscopy—electron backscatter diffraction (SEM-EBSD) shows recovery (subgrains) and recrystallization as well as mineral inclusions due to the metamorphic history (Mamtani *et al.* 2023), but no oxidation. X-ray absorption near edge structure (XANES) analysis of iron oxidation states shows only a slight change at high shock pressure. After shock, part of the samples were heat-treated to 973 K to exceed T_C in an argon atmosphere to prevent oxidation (Kontny *et al.* 2018). The pure magnetite composition is confirmed by a Curie temperature of $T_C = 861 \pm 2$ K for all samples.

The experimental χ-T curves are shown in Fig. 1(a). After shock ≥ 5 GPa, T_V is increased by about 5 K (Table 1) and the susceptibility at temperatures above the transition is significantly lower (Kontny *et al.* 2018). Reheating causes a recovery of the shock-induced changes towards the initial state. Similarly, hysteresis measurements showed a decrease in saturation magnetization M_s after shock and an increase after reheating (Kontny *et al.* 2018). The hysteresis measurements indicate that the initial sample is in the range of multidomain (MD) behaviour. After shock, the authors identified pseudo-single domain (PSD) behaviour with a tendency to MD behaviour after reheating. Changes in domain state are more pronounced at higher shock pressures. Reznik *et al.* (2016) identified grain fragmentation, lattice defects and micro-shear bands indicating inhomogeneously distributed brittle and plastic deformation.
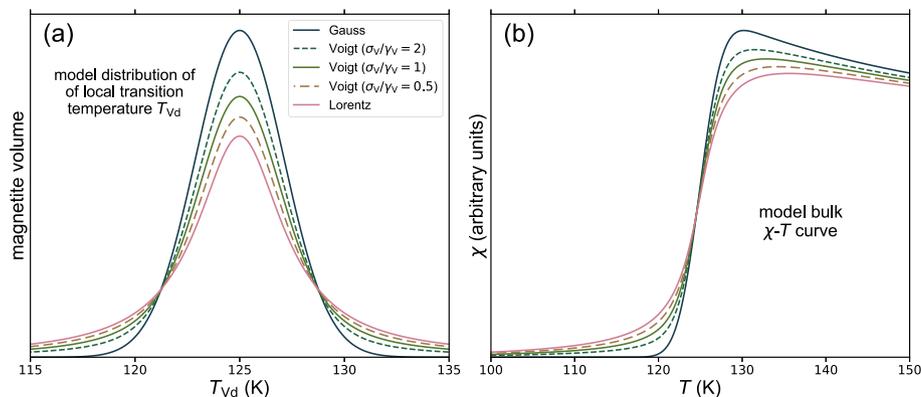
Figure 3. (a) Distribution of T_{Vd} over the magnetite volume fractions for different ratios of σ_V/γ_V. (b) Bulk χ-T curves resulting from the distributions shown in (a). The curves represent the sum of the χ contributions of the local transition temperatures. Model parameters: $\bar{T}_V = 125$ K; $r_{1d} = 0.035$; $c_{1d} = 0.3$; $FWHM_{Voigt} = 5$ K.
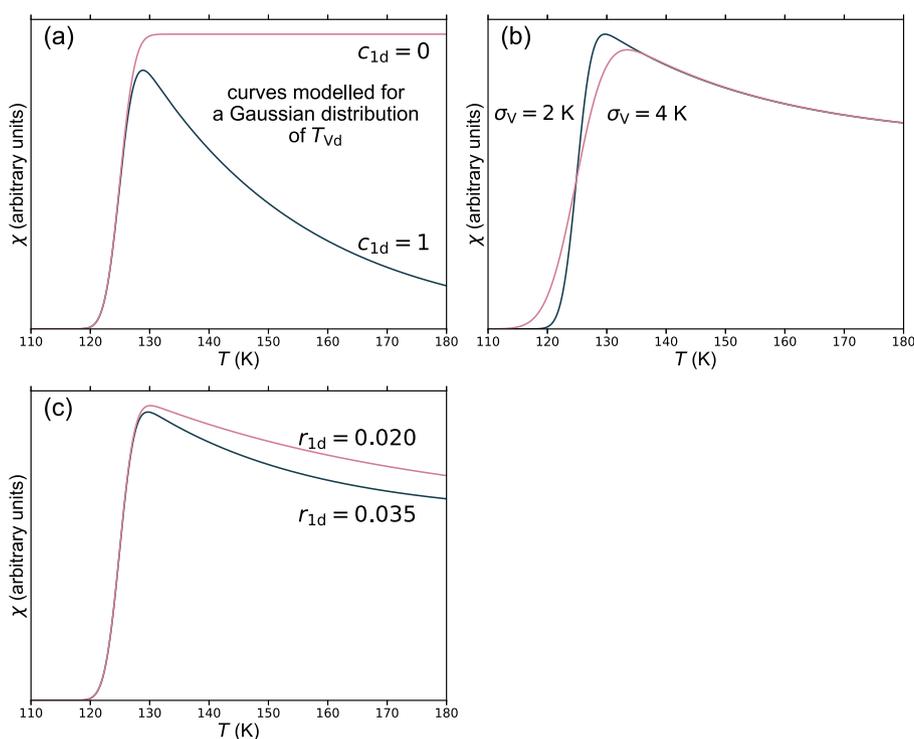
Figure 4. Changes in the bulk χ-T curve by varying individual parameters for a Gaussian distribution. Unless indicated in the figures, the following parameters were used: $\bar{T}_V = 125$ K; $r_{1d} = 0.035$; $\sigma_V = 2$ K; $\gamma_V = 0$ K; $c_{1d} = 0.4$. Variations of (a) c_{1d} (temperature-dependent fraction of χ at T_{Vd}); (b) σ_V (scale parameter of the distribution of T_{Vd}) and (c) r_{1d} (rate of the exponential susceptibility decrease).

Table 1. Parameters from the evaluation of the measured magnetite χ-T curves before heat treatment assuming a Voigt profile for the distribution of T_{Vd}. [1]Data from Kontny *et al.* (2018). [2]Standard deviation σ between the model susceptibility and the normalized χ-T curve.

Sample	T_V (K) [1]	$\bar{T}_V$ (K)	σ_V (K)	γ_V (K)	*glmix*	$FWHM_{Voigt}$ (K)	c_{1d} (-)	r_{1d} (-)	σ (-) [2]
Initial	118	119.9	0.0	0.6	1.00	1.2	0.27	0.034	1.1×10^{-4}
3 GPa	119	121.7	0.0	0.7	1.00	1.5	0.23	0.024	1.0×10^{-4}
5 GPa	123	125.5	2.9	0.5	0.12	7.3	0.47	0.020	3.7×10^{-4}
10 GPa	123	124.5	1.1	3.3	0.72	7.5	0.59	0.025	3.3×10^{-4}
20 GPa	122	124.7	1.4	2.8	0.64	7.2	0.55	0.026	3.6×10^{-4}
30 GPa	122	124.1	2.3	1.8	0.40	7.7	0.50	0.024	3.3×10^{-4}

The authors also reported lattice distortion induced by the shock wave associated with elastic strain. Reznik *et al.* (2016) reported an inhomogeneous distribution of deformation features in all shocked samples with pressure-dependent variations in the identified features of brittle and plastic deformation.

The shock reverberation experiments were performed at the Ernst–Mach–Institute in Freiburg (Germany). Detailed information about the experimental setup and the method are given in Müller & Hornemann (1969), Fritz *et al.* (2011) and Reznik *et al.* (2016). The samples were shocked at maximum pressures of 3, 5, 10, 20 and 30 GPa. Up to 10 GPa, an air gun was used to accelerate a flyer plate for momentum transfer on the sample. For higher pressures, high explosives were used to accelerate the flyer plate. The Hugoniot elastic limit (HEL) of magnetite was exceeded for at least 5 GPa shock pressure, resulting in both brittle and plastic deformation (Reznik *et al.* 2016). After shock at 3 GPa, no significant changes in domain state from the initial magnetite were observed, indicating that the HEL was not yet reached (Mendes & Kontny 2024).

The low-temperature susceptibility measurements were performed with an AGICO KLY-4S Kappabridge (effective field intensity: 300 A m^{-1}; frequency: 875 Hz) equipped with a CS-L low-temperature cryostat (83–300 K). The accuracy of the recorded temperature is within ± 1 K (according to thermometer supplier JUMO) and the displayed resolution is 0.1 K. The sample is placed in a test tube with the cryostat cooled with liquid nitrogen. After purging the nitrogen with argon, χ is measured in ambient atmosphere while warming to room temperature. Measurement with the AGICO KLY-4S instrument is described by Pokorný *et al.* (2004).

3 APPLICATION OF THE MODEL TO χ-T DATA OF SHOCKED AND REHEATED MAGNETITE ORE

The full width at half maximum ($FWHM_{\text{Voigt}}$) is determined to quantify the transition width. The $FWHM$ of a Gaussian distribution is $FWHM_{\text{Gauss}} = 2\sigma_V\sqrt{2\ln 2}$ and the $FWHM$ of a Lorentzian distribution is $FWHM_{\text{Lorentz}} = 2\gamma_V$. The $FWHM$ of the Voigt profile is approximated using an approach of Whiting (1968), modified by Olivero & Longbothum (1977):

$$FWHM_{\text{Voigt}} \approx 0.5346\, FWHM_{\text{Lorentz}} + \sqrt{0.2166\, FWHM_{\text{Lorentz}}^2 + FWHM_{\text{Gauss}}^2}. \tag{8}$$

Major *et al.* (2020) introduced $glmix = FWHM_{\text{Lorentz}}/(FWHM_{\text{Lorentz}} + FWHM_{\text{Gauss}})$ to characterize the Voigt profile. The parameter varies between 0 for pure Gaussian and 1 for pure Lorentzian.

The parameters obtained, assuming a Voigt profile, are shown before heat treatment (Table 1) and after heat treatment (Table 2). Results for a Gaussian and Lorentzian distribution are shown in the supplements. For comparison, T_V, determined by the maximum of dχ/dT given in Kontny *et al.* (2018), is shown. For the magnetite ore shocked at 10 GPa, $glmix = 0.72$ was determined for the Voigt profile (Fig. 5), corresponding to a predominantly Lorentzian distribution. The differences resulting from using a Voigt profile or a Lorentzian distribution of T_{Vd} are insignificant at 10 GPa and both accurately describe the experimental observations. In contrast, the best Gaussian fitting does not adequately describe the measured curve, especially the rather flat susceptibility increase at low temperatures The quality of the fits was assessed by the standard deviation σ between the model susceptibility and the normalized χ-T curve over the whole measured temperature range ($\sigma_{\text{Gauss,10GPa}} = 8.3 \times 10^{-3}$, $\sigma_{\text{Lorentz,10GPa}} = 3.4 \times 10^{-4}$, $\sigma_{\text{Voigt,10GPa}} = 3.3 \times 10^{-4}$).

4 INTERPRETATION

4.1 Effect of shock and heat treatment

The measured χ-T curves of the initial, 3, 5 and 10 GPa magnetite ore before and after heat treatment are shown in Figs 6(a)–(d) along with the best approximation for a Voigt profile. The χ-T curves for 20 and 30 GPa are similar to the 10 GPa curve (see Fig. 1). All measured χ-T curves were well approximated with a Voigt profile over the entire temperature range. The corresponding distributions of T_{Vd} over the magnetite volume are shown before heat treatment (Fig. 6e) and after heat treatment (Fig. 6f). The initial and 3 GPa magnetite ore show a narrow, almost pure Lorentzian distribution, which changes to a narrow Gaussian distribution after heat treatment (see Tables 1 and 2). The change towards a Lorentzian character is reflected by a smaller susceptibility increase below $\bar{T}_V$ (Figs 6a and b).

The $\bar{T}_V$ of the initial (120 K) and 3 GPa magnetite ore (122 K) is within the typical range of T_V for stoichiometric magnetite with low internal stress. At 5 GPa and above, shock causes a large increase in transition width, which varies little with shock pressure (Fig. 6e). For these samples, $\bar{T}_V$ is approximately 125 K. After heating, $\bar{T}_V$ is between 121 and 123 K for all samples, with a slight increase at pressures below the HEL and a slight decrease above. These differences are within the uncertainty of the Kappabridge measurements.

4.2 Shock pressure dependence of the Verwey transition

The changes in $\bar{T}_V$, which is the centre of the distribution of T_{Vd}, the transition width ($FWHM$) and c_{1d} of the shocked and subsequently heat-treated magnetite are compared with the results of Reznik *et al.* (2016) and Kontny *et al.* (2018) in Figs 7(a)–(f). The pressure dependence of $\bar{T}_V$ (Fig. 7a) and T_V (Fig. 7b), determined from the maximum of dχ/dT (Kontny *et al.* 2018), are similar. However, the slight decrease in T_V at 20 and 30 GPa was not observed with the current model, which may be due to uncertainties in the different evaluation procedures.

Figs 7(c) and (d) compare the model transition width of the shocked samples with the results of Reznik *et al.* (2016) from fitting a Gaussian distribution to dχ/dT around T_V. Assuming a Gaussian distribution of T_{Vd}, the shock pressure dependence of the $FWHM$ is very similar to the model results, showing a maximum at 10 GPa and a slight decrease at higher shock pressures. A Gaussian distribution cannot describe the flat susceptibility increase from 80 K upwards (see Fig. 5) and therefore the increase does not significantly affect the $FWHM$ compared to the determination based on dχ/dT. Assuming a Voigt profile, the $FWHM$ of the shocked magnetite ore is significantly lower and more independent of shock pressure. Since the Voigt profile allows an accurate fitting at low temperatures, it follows that the inclusion of low-temperature susceptibility does not cause an increase in the $FWHM$, but a change from a Gaussian to a more Lorentzian character. At 3 GPa, the transition width is not significantly affected by shock and heat treatment. After heat treatment, the transition width in shocked magnetite decreases but remains above that of the initial magnetite ore.

Table 2. Parameters from the evaluation of the measured magnetite χ-T curves after heat treatment assuming a Voigt profile for the distribution of $T_{\mathbf{Vd}}$. [1]: Data from Kontny *et al.* (2018). [2]: Standard deviation σ between the model susceptibility and the normalized χ-T curve.

Sample	T_V (K) [1]	$\bar{T}_V$ (K)	σ_V (K)	γ_V (K)	*glmix*	$FWHM_{Voigt}$ (K)	c_{1d} (-)	r_{1d} (-)	σ (-) [2]
Initial	121	121.9	1.2	0.1	0.04	3.0	0.17	0.034	2.6×10^{-4}
3 GPa	120	122.7	0.7	0.5	0.37	2.3	0.29	0.022	2.5×10^{-4}
5 GPa	120	122.0	1.5	0.3	0.14	3.8	0.29	0.021	3.3×10^{-4}
10 GPa	120	122.1	1.8	0.5	0.18	4.7	0.30	0.023	3.6×10^{-4}
20 GPa	119	121.1	1.9	0.6	´0.20	5.0	0.29	0.024	3.1×10^{-4}
30 GPa	121	122.5	1.7	0.7	0.26	4.9	0.32	0.025	3.5×10^{-4}
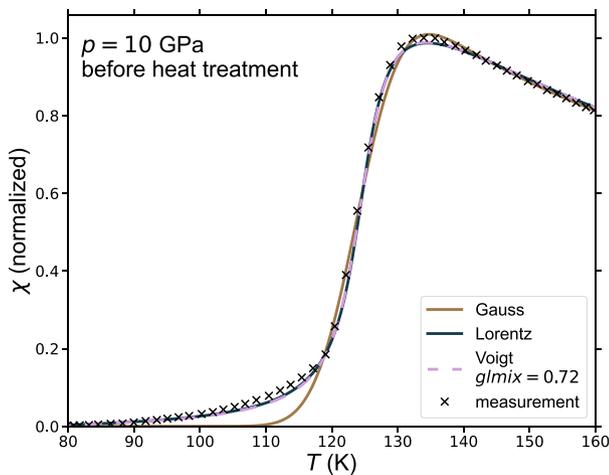
Figure 5. -T curve of magnetite ore after shock at 10 GPa (x). Best fits for a Gaussian distribution, a Lorentzian distribution and a Voigt profile for the distribution of $T_{\mathbf{Vd}}$ are shown.

Similar to $T_V P = \chi_{max}/\chi_{10°\,C}$ (Kontny *et al.* 2018), c_{1d} depends on the ratio of the susceptibility at ambient temperature to the maximum near the isotropic point. After shock and after heat treatment, c_{1d} (Fig. 7e) and $T_V P$ (Fig. 7f) show a similar dependence on shock pressure. The larger relative decrease in susceptibility after shock is reflected by an increase in c_{1d} for pressures above the HEL. The increase is largest at 10 GPa. Heat treatment causes a strong recovery of c_{1d} in magnetite ore, shocked above the HEL, to the value of the 3 GPa magnetite ore. A decrease of c_{1d} was also observed in the original magnetite.

For a linear representation of the distribution character, *glmix* (Major *et al.* 2020) is shown (Fig. 7g). Except for 5 GPa, where the distribution character is Gaussian both after shock and after heat treatment, the pressure dependence of *glmix* shows a clear trend. Without shock at pressures below the HEL, the character is almost pure Lorentzian before heat treatment. From 10 GPa onwards, the character becomes increasingly Gaussian. Heat treatment causes a shift towards a more Gaussian character for all samples except 5 GPa. The change is largest in the original magnetite, which shows an almost pure Gaussian character after heat treatment, whereas the magnetite subjected to the highest shock pressures retains a more Lorentzian character. The 3 GPa sample has a slightly more Lorentzian character, probably related to the small transition width, which increases the uncertainty of the determination.

A higher value of the exponential decrease rate r_{1d} indicates that the initial magnetite ore shows a significantly stronger susceptibility decrease above the isotropic point both before and after heating than the shocked samples (Fig. 7h). Heat treatment and shock pressure

variations have no clear effect on r_{1d}, although r_{1d} is slightly lower at 5 GPa, close to the HEL.

5 DISCUSSION

5.1 Shock and heat-induced changes of low-temperature behaviour and transition shape

Low-temperature χ-T curves of a tectonically deformed magnetite ore, shocked between 3 and 30 GPa and later heat-treated up to 973 K, show strong variations, especially near the Verwey transition. Reznik *et al.* (2016) and Kontny *et al.* (2018) suggested that the parameters calculated from these curves contain information on magnetic domain state. For these particular samples, the differences are interpreted in terms of different strain and lattice defects and annealing.

Magnetic susceptibility from about 80 to 280 K is numerically approximated under the assumption of a probability distribution of local transition temperatures T_{Vd} within the bulk magnetite. This approach considers the decrease in magnetic susceptibility above the Verwey transition for the shape approximation, unlike methods that use dχ/dT to determine T_V (e.g. Reznik *et al.* 2016; Kontny *et al.* 2018). The extended fitting range improves the description of the shape and transition width with a minor effect on the determination of T_V. By using a distribution of T_{Vd}, thermal variations of the bulk susceptibility near the Verwey transition affect the parameter determination and increase the accuracy. The numerical approximation describes the measured curves well, even above T_V, where both the transition and the decrease related to magnetocrystalline anisotropy might affect the susceptibility. At temperatures well above the transition, the model curve is controlled by the exponential decrease corresponding to variations in magnetocrystalline anisotropy.

On a microscopic scale, the processes associated with the Verwey transition are complex. Interactions between monoclinic twin walls and magnetic domain walls that characterize the transition are strongly influenced by, for example, dislocation structures and therefore cause sensitivity to deformation (e.g. Kasama *et al.* 2010; Lindquist *et al.* 2019). The idealization by an instantaneous susceptibility increase in a homogeneous volume does not reflect these processes, but allows a good characterization of the bulk behaviour without increasing the complexity of the model. The samples can be well approximated with a single temperature distribution. A change in processes controlling the susceptibility below T_V, namely variations of the magnetization in the monoclinic phase (Kosterov 2003) and the transition to the cubic phase, can be suspected but is not visible in the χ-T behaviour. It is suggested that both processes are controlled by shock-induced internal stresses. Kosterov & Fabian (2008) assumed that
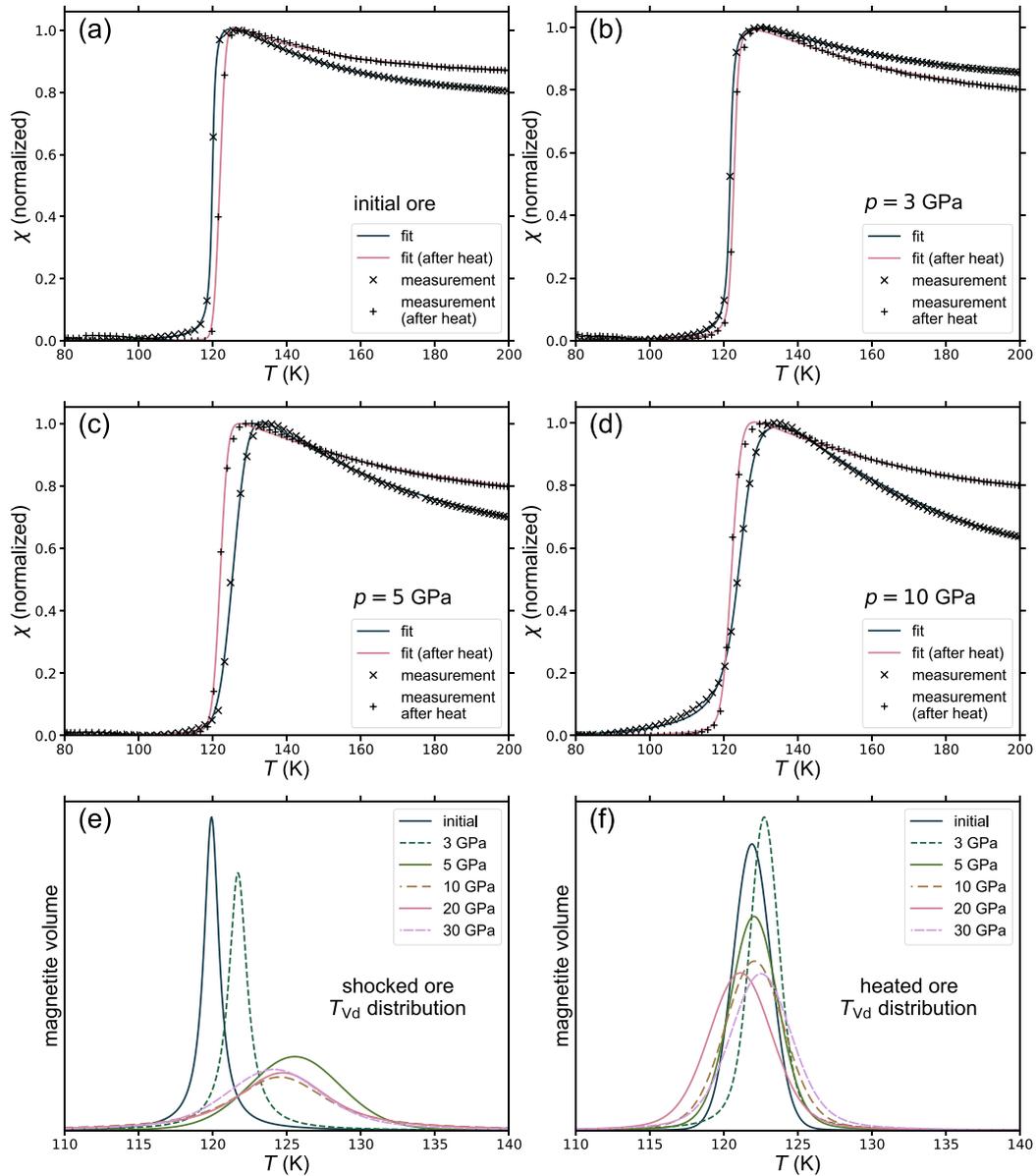
Figure 6. Measured χ-T curves before (x) and after heat treatment (+) and best Voigt fittings before and after heat treatment: (a) initial ore without shock, (b) shock pressure 3 GPa, (c) 5 GPa, (d) 10 GPa. (e) Model distributions of local transition temperatures T_{Vd} before and (f) after heat treatment. The distributions are normalized to the same area, resulting in variations in peak height depending on the *FWHM* and type of distribution.

defect-related internal stresses cause pinning of monoclinic twin boundaries.

The centre $\bar{T}_V$ of the distribution of T_{Vd} is interpreted as an average value during warming through the transition, corresponding to T_V determined for bulk magnetite. The values of $\bar{T}_V$ are close to T_V determined by Kontny *et al.* (2018). The *FWHM* of the model distribution is a measure of the transition width. The *FWHM* corresponds to the spread of T_{Vd} in the bulk magnetite and reflects the distribution of internal stress. The difference between the transition width determined by Reznik *et al.* (2016) and Kontny *et al.* (2018) and the distribution width of T_{Vd} is small. Especially at shock pressures above the HEL, variations in internal stress state can be attributed to dislocations. The sharp transition in initial magnetite and magnetite shocked below the HEL is consistent with the stoichiometric composition and pre-existing tectonic deformation (Reznik *et al.* 2016; Mamtani *et al.* 2023). The broad transition above the HEL could

be interpreted as an increase of microstress in magnetite associated with a higher dislocation density.

The strong shock-induced susceptibility variations together with the high susceptibility of the magnetite ore allow to distinguish between a Gaussian and Lorentzian character of a Voigt profile. Variations in the distribution character are mainly attributed to outliers of T_{Vd} and not to the distribution width (e.g. Succi & Coveney 2019). The Lorentzian distribution character of the initial magnetite ore indicates a correlation of T_{Vd} caused by internal stress associated with tectonic deformation, which is not significantly altered by shock up to 3 GPa. Slightly above the HEL (5 GPa), the transition width is broadened without the low-temperature susceptibility increase observed after shock at higher pressures, resulting in a Gaussian character, that may indicate a more brittle deformation. The behaviour at 5 GPa may be related to differences in the dominant deformation mechanisms, or to a more
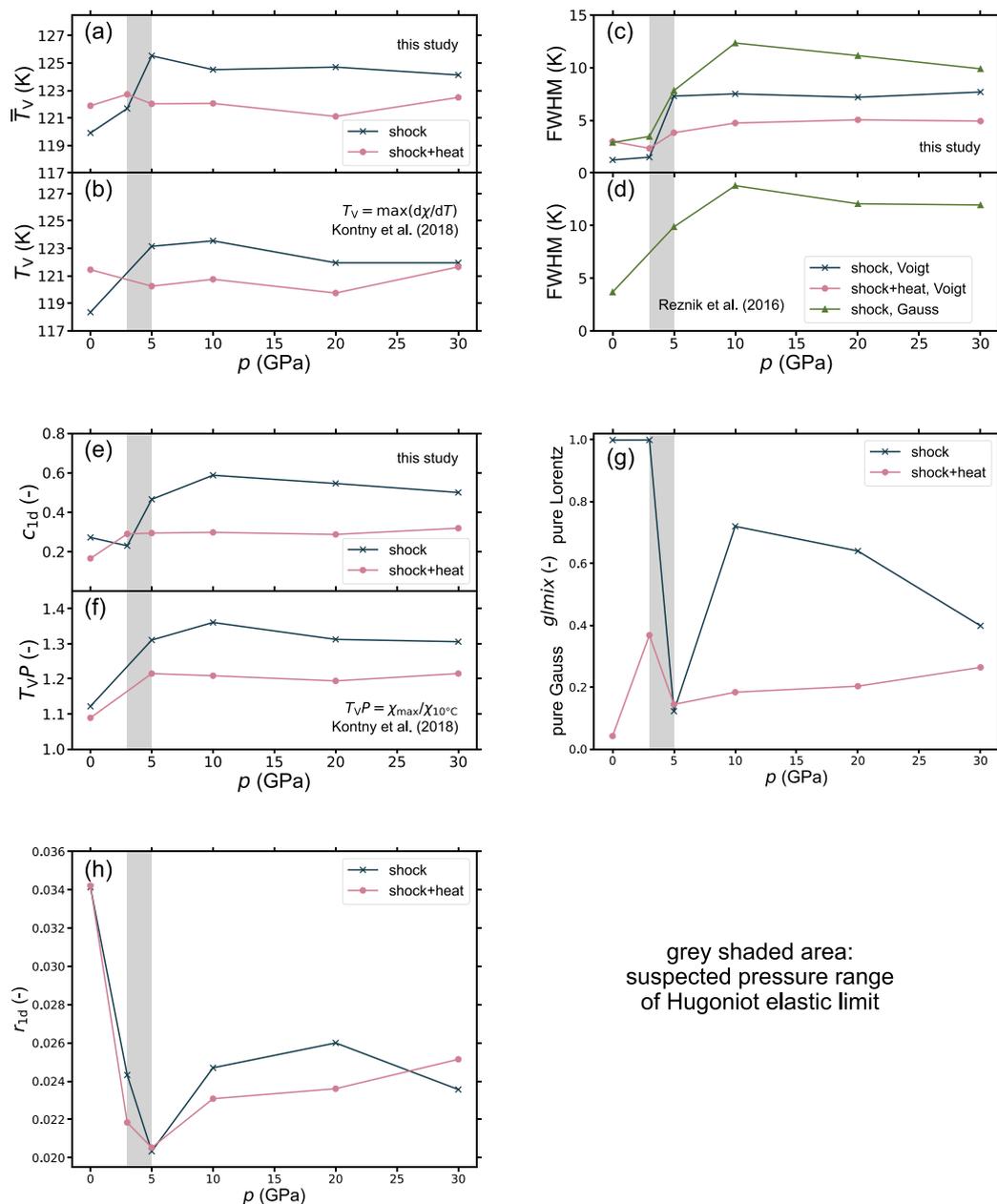
Figure 7. Pressure dependence of model parameters after shock and subsequent heat treatment of magnetite. The suspected range of the HEL between 3 and 5 GPa is shown. Unless otherwise stated, the fittings are made for a Voigt profile. For comparison, related parameters for the same χ-T curves from Reznik et al. (2016), Kontny et al. (2018) are shown. (a) $\bar{T}_V$; (b) T_V (Kontny et al. 2018); (c) *FWHM*: shock (Gaussian distribution, Voigt profile); shock and heat (Voigt profile); (d) *FWHM*: shock, Gaussian distribution (Reznik et al. 2016) (e) c_{1d}; (f) $T_V P$ (Kontny et al. 2018); (g) distribution character $glmix$; (h) rate of exponential susceptibility decrease r_{1d}.

heterogeneous dislocation distribution. Above the HEL the internal stress field is expected to be strongly influenced by dislocations. The increasingly Gaussian character after shock at highest pressures indicates a more random distribution of internal stresses, presumably related to dislocation annealing by shock-induced heating (e.g. Tong *et al.* 2015). The occurrence of higher temperatures due to higher shock pressures is supported by microstructural observations, such as local amorphization (Reznik *et al.* 2016). Reheating caused a shift towards a Gaussian character after shock both below and above the HEL, indicating further annealing. This is supported by a decrease in coercivity H_c (Kontny *et al.* 2018). The

smaller shift in magnetite deformed at the highest shock pressures suggests that a larger fraction of dislocations cannot be annealed or that deformation features like deformation twins are harder to anneal.

One might speculate that plastic deformation at shock pressures beyond the HEL causes the formation of subgrains smaller than the original magnetic domains. After heating, dislocations could persist at interfaces between recrystallized subgrains and be related to the lower susceptibility. A change from multidomain to vortex-state and a stable single magnetic domain grain size can be seen as a major reason for the decrease in magnetic susceptibility (Mendes

& Kontny 2024). The shock pressure and impact heat cause a fragmentation (shock wave) and partial annealing of internal stresses during the shock.

Verwey transition temperatures of magnetite in crystalline rocks are mainly between about 100 and 125 K, rarely exceeding 130 K (Jackson & Moskowitz 2021). Even after shock, $\bar{T}_V$ does not exceed 126 K, and only a small proportion of T_{Vd} is about 130 K. Therefore, the results obtained are plausible, although no upper bound on T_{Vd} was defined. Bimodal distributions of T_V are observed in many rocks and can be interpreted in several ways, e.g. as significant distinct magnetite populations or caused by a discontinuity in T_V beyond a critical point of non-stoichiometry (Jackson & Moskowitz 2021). First tests indicate that the presented approach is suitable for unmixing bimodal distributions of transition temperatures. Numerical unmixing of overlapping peaks is also used to separate contributions from different magnetic materials in coercivity spectra (e.g. Heslop 2015). Fitting of overlapping peaks is a common issue in the interpretation of Mössbauer spectra of Fe-bearing minerals (e.g. Dyar *et al.* 2006). Thermodynamic calculations by Coe *et al.* (2012) indicate that dT_V/dp can exceed 10 K GPa^{-1} under directional strain in agreement with observations by Nagasawa *et al.* (2007). After shock above 10 GPa, the susceptibility increases already at the lower measurement limit (80 K). However, these changes may be caused not only by a linear strain relation, but also by processes in the monoclinic phase or additional effects such as lattice distortion or changes in local stoichiometry.

5.2 Susceptibility variations between the Verwey transition and room temperature

For PSD to MD magnetite grains, the susceptibility decrease between the Verwey transition and room temperature is inversely related to the thermal variation of the magnetocrystalline anisotropy (Muxworthy 1999). Therefore, our model describes the decrease above T_{Vd} by a temperature-dependent susceptibility $\chi_{1d}(T)$. The rate r_{1d} of the exponential approach describing the susceptibility decrease is high in the tectonically deformed initial magnetite, compared to shocked and reheated magnetite. This indicates a stronger increase of the magnetocrystalline anisotropy near the isotropic point for the tectonically deformed MD magnetite. Shock deformation seems to reduce the development of a magnetocrystalline anisotropy in line with a higher dislocation density and reduced magnetic grain sizes. However, r_{1d} is rather invariant to shock pressure variations and reheating, with slightly lower values close to the HEL (5 GPa).

The relative susceptibility loss at room temperature, quantified by c_{1d}, is sensitive to shock deformation and reheating. After shock above the HEL, high values of c_{1d} reflect a high relative susceptibility loss. Analogous to the variations of the transition shape (*FWHM*, *glmix*), the susceptibility loss is largest at 10 GPa and heat treatment causes a partial recovery. A relative decrease in room temperature susceptibility after manual powdering of a natural magnetite single crystal (Fig. 8) suggests a relation to grain refinement. Therefore, the increase in c_{1d} may be related to shock-induced grain fragmentation, consistent with the interpretation of Kontny *et al.* (2018). These authors observed an increase in crystallite size after heat treatment, consistent with the decrease of c_{1d}. The reduction in c_{1d} in heated initial magnetite suggests a sensitivity to tectonic lattice strain.

The susceptibility decrease is well described by the exponential approach. The susceptibility is almost constant at the upper fitting
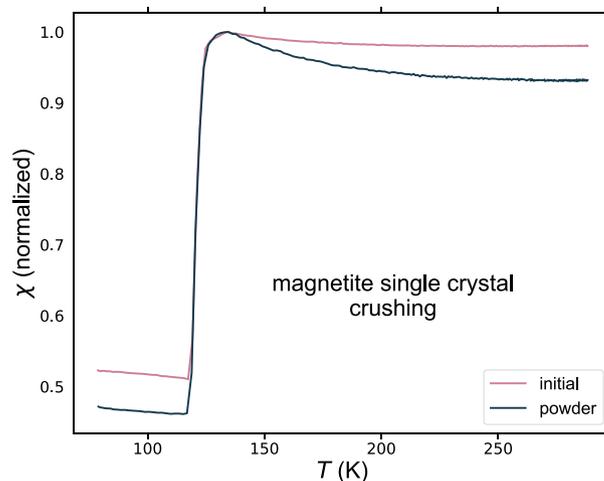
Figure 8. Measured χ-T curves of a natural magnetite single crystal before and after manual crushing.

limit (280 K) and c_{1d} can therefore be accurately determined. A significant mutual influence in the determination of r_{1d} and c_{1d} is therefore unlikely, although both describe the same temperature range.

6 CONCLUSIONS

The presented model allows a quantitative numerical analysis of susceptibility variations from the Verwey transition up to 280 K in magnetite-bearing rocks. In this study, it is applied to a well-characterized magnetite ore that exhibits strong variations in low-temperature susceptibility related to experimental shock and heating. The model includes parameters for the characterization of important features such as T_V, the transition width and the relative susceptibility decrease up to room temperature. A distribution of local transition temperatures T_{Vd} in bulk magnetite is assumed. For the particular setting, T_{Vd} is expected to be strongly influenced by internal stress fields.

Voigt profiles, which can have a Gaussian or Lorentzian character, are used for the numerical description of the distribution. The Gauss/Lorentz character shows high sensitivity to shock and heat treatment or to a defect-rich or defect-poor crystal lattice, respectively. A Lorentzian character indicates a local correlation of T_{Vd} with more outliers, suggesting a higher amount of dislocations related to internal stress fields. This behaviour is related to plastic deformation under high shock pressures and a reduction of magnetic domain size. A Gaussian character suggests no correlation between the local transition temperatures T_{Vd} in the bulk magnetite, which can be interpreted as a decrease in internal stresses due to annealing.

The susceptibility decrease above T_V, which can be related to the decrease of the magnetocrystalline anisotropy constant K_1 of magnetite in this temperature range (e.g. Muxworthy & McClelland 2000), is well described with an exponential temperature dependence for the analysed magnetite ore. The results support the main findings of Reznik *et al.* (2016) and Kontny *et al.* (2018) of strong shock-induced deformation and annealing effects at high shock temperatures and subsequent heat treatment, and allow a more detailed evaluation of the effect of internal strain (lattice defects) and internal elastic stress on the magnetic behaviour around the Verwey transition.

The approach could be applied to other magnetite-bearing rocks where a detailed description of the Verwey transition shape is considered useful. Application to curves with a more pronounced susceptibility peak at the isotropic point, or significant cation substitution, or oxidation may require adjustments to the model.

ACKNOWLEDGMENTS

SUPPORTING INFORMATION

Supplementary data are available at *GJI* online.

supplement_1.txt

Please note: Oxford University Press is not responsible for the content or functionality of any supporting materials supplied by the authors. Any queries (other than missing material) should be directed to the corresponding author for the paper.

DATA AVAILABILITY

The data underlying this article are available in the KITopen repository, at https://dx.doi.org/10.35097/hbwBDGIgWbcvTFYc.

REFERENCES

Aragón, R., Buttrey, D.J., Shepherd, J.P. & Honig, J.M., 1985. Influence of nonstoichiometry on the Verwey transition, *Phys. Rev. B,* **31**(1), 430–436.

Armstrong, B.H., 1967. Spectrum line profiles: the Voigt function, *J. Quant. Spectrosc. Radiat. Transfer,* **7**(1), 61–88.

Biało, I. *et al.*, 2019. The influence of strain on the Verwey transition as a function of dopant concentration: towards a geobarometer for magnetite-bearing rocks, *Geophys. J. Int.,* **219**(1), 148–158.

Bickford, L.R., Brownlow, J.M. & Penoyer, R.F., 1957. Magnetocrystalline anisotropy in cobalt-substituted magnetite single crystals, *Proc. IEEE—Part B: Radio Electr. Eng.,* **104**(5S), 238–244.

Brabers, V.A.M., Walz, F. & Kronmüller, H., 1998. Impurity effects upon the Verwey transition in magnetite, *Phys. Rev. B,* **58**(21), 14163–14166.

Calhoun, B.A., 1954. Magnetic and electric properties of magnetite at low temperatures, *Phys. Rev.,* **94**(6), 1577–1585.

Carporzen, L. & Gilder, S.A., 2010. Strain memory of the Verwey transition, *J. geophys. Res.,* **115**(B5), doi:10.1029/2009JB006813.

Carporzen, L., Gilder, S.A. & Hart, R.J., 2006. Origin and implications of two Verwey transitions in the basement rocks of the Vredefort meteorite crater, South Africa, *Earth planet. Sci. Lett.,* **251**(3-4), 305–317.

Coe, R.S., Egli, R., Gilder, S.A. & Wright, J.P., 2012. The thermodynamic effect of nonhydrostatic stress on the Verwey transition, *Earth planet. Sci. Lett.,* **319-320,** 207–217.

Csikor, F.F. & Groma, I., 2004. Probability distribution of internal stress in relaxed dislocation systems, *Phys. Rev. B,* **70**(6), doi:10.1103/PhysRevB.70.064106.

Dyar, M.D., Agresti, D.G., Schaefer, M.W., Grant, C.A. & Sklute, E.C., 2006. Mössbauer spectroscopy of Earth and Planetary Materials, *Annu. Rev. Earth planet. Sci.,* **34**, 83–125.

Fritz, J., Wünnemann, K., Reimold, W.U., Meyer, C. & Hornemann, U., 2011. Shock experiments on quartz targets pre-cooled to 77 K, *Int. J. Impact Eng.,* **38**(6), 440–445.

Gasparov, L. *et al.*, 2005. Magnetite: raman study of the high-pressure and low-temperature effects, *J. appl. Phys.,* **97**(10), doi:10.1063/1.1854476.

Gasparov, L., Shirshikova, Z., Pekarek, T.M., Blackburn, J., Struzhkin, V., Gavriliuk, A., Rueckamp, R. & Berger, H., 2012. Raman study of the Verwey transition in magnetite at high-pressure and low-temperature: effect of Al doping, *J. Appl. Phys.,* **112**(4), 043510, doi:10.1063/1.4747834.

Heslop, D., 2015. Numerical strategies for magnetic mineral unmixing, *Earth Sci. Rev.,* **150,** 256–284.

Honig, J.M., 1995. Analysis of the Verwey transition in magnetite, *J. Alloys Compd.,* **229**(1), 24–39.

Hunt, C.P., Moskowitz, B.M. & Banerjee, S.K., 1995. Magnetic properties of rocks and minerals, in *Rock Physics and Phase Relations: a Handbook of Physical Constants,* Vol. **3**, pp. 189–204, ed. Ahrens, Thomas J., AGU.

Jackson, M.J. & Moskowitz, B., 2021. On the distribution of Verwey transition temperatures in natural magnetites, *Geophys. J. Int.,* **224**(2), 1314–1325.

Johnson, S.G., 2012. Faddeeva W function implementation. viewed 21 February 2024, from http://ab-initio.mit.edu/Faddeeva.

Kąkol, Z., Sabol, J., Stickler, J. & Honig, J.M., 1992. Effect of low-level titanium(IV) doping on the resistivity of magnetite near the Verwey transition, *Phys. Rev. B,* **46**(4), 1975–1978.

Kakudate, Y., Mori, N. & Kino, Y., 1979. Pressure effect on the anomalous electrical conductivity of magnetite, *J. Magn. Magn. Mater.,* **12**(1), 22–25.

Kasama, T., Church, N.S., Feinberg, J.M., Dunin-Borkowski, R.E. & Harrison, R.J., 2010. Direct observation of ferrimagnetic/ferroelastic domain interactions in magnetite below the Verwey transition, *Earth planet. Sci. Lett.,* **297**(1-2), 10–17.

Kontny, A. & Grothaus, L., 2017. Effects of shock pressure and temperature on titanomagnetite from ICDP cores and target rocks of the El'gygytgyn impact structure, Russia, *Stud. Geophys. Geod.,* **61,** 162–183.

Kontny, A., Reznik, B., Boubnov, A., Göttlicher, J. & Steininger, R., 2018. Postshock thermally induced transformations in experimentally shocked magnetite, *Geochem. Geophys. Geosyst.,* **19**(3), 921–931.

Kosterov, A., 2003. Low-temperature magnetization and AC susceptibility of magnetite: effect of thermomagnetic history, *Geophys. J. Int.,* **154**(1), 58–71.

Kosterov, A. & Fabian, K., 2008. Twinning control of magnetic properties of multidomain magnetite below the Verwey transition revealed by measurements on individual particles, *Geophys. J. Int.,* **174**(1), 93–106.

Kozłowski, A., Kąkol, Z., Kim, D., Zalecki, R. & Honig, J.M., 1996a. Heat capacity of Fe$_3$- alpha M alpha O$_4$ (M=Zn, Ti, $0 <\sim$ alpha $<\sim 0.04$), *Phys. Rev. B,* **54**(17), doi:10.1103/physrevb.54.12093.

Kozłowski, A., Metcalf, P., Kąkol, Z. & Honig, J.M., 1996b. Electrical and magnetic properties of Fe$_{3-z}$Al$_z$O$_4$ ($z<0.06$). *Phys. Rev. B,* **53**(22), doi:10.1103/PhysRevB.53.15113.

Lindquist, A.K., Feinberg, J.M., Harrison, R.J., Loudon, J.C. & Newell, A.J., 2015. Domain wall pinning and dislocations: investigating magnetite deformed under conditions analogous to nature using transmission electron microscopy, *J. geophys. Res.,* **120**(3), 1415–1430.

Lindquist, A.K., Feinberg, J.M., Harrison, R.J., Loudon, J.C. & Newell, A.J., 2019. The effects of dislocations on crystallographic twins and domain wall motion in magnetite at the Verwey transition, *Earth, Planets, Space,* **71**, 5, doi:10.1186/s40623-018-0981-7.

Major, G.H., Fairley, N., Sherwood, P.M.A., Linford, M.R., Terry, J., Fernandez, V. & Artyushkova, K., 2020. Practical guide for curve fitting in x-ray photoelectron spectroscopy, *J. Vac. Sci. Technol. A,* **38**(6), doi:10.1116/6.0000377.

Mamtani, M.A., Wenzel, O., Kontny, A., Hilgers, C., Müller, E., Renjith, A.R., Llorens, M.-G. & Gomez-Rivas, E., 2023. "In-plane" site-specific FIB lamella extraction from deformed magnetite and the investigation of low angle grain boundaries under TEM, *J. Struct. Geol.,* **174,** doi:10.1016/j.jsg.2023.104937.

Mang, C. & Kontny, A., 2013. Origin of two Verwey transitions in different generations of magnetite from the Chesapeake Bay impact structure, USA, *J. geophys. Res.,* **118**(10), 5195–5207.

Mendes, B.D.L. & Kontny, A., 2024. Restoration and transformation: the response of shocked and oxidized magnetite to temperature, *J. geophys. Res.,* **129**(2), e2023JB027244.

Moskowitz, B.M., 1993. Micromagnetic study of the influence of crystal defects on coercivity in magnetite, *J. geophys. Res.,* **98**(B10), 18 011–18 026.

Müller, W.F. & Hornemann, U., 1969. Shock-induced planar deformation structures in experimentally shock-loaded olivines and in olivines from chondritic meteorites, *Earth planet. Sci. Lett.,* **7**(3), 251–264.

Muramatsu, T., Gasparov, L.V., Berger, H., Hemley, R.J. & Struzhkin, V.V., 2016. Electrical resistance of single-crystal magnetite (Fe3O4) under quasi-hydrostatic pressures up to 100 GPa, *J. appl. Phys.,* **119**(13), doi:10.1063/1.4945388.

Muxworthy, A.R., 1999. Low-temperature susceptibility and hysteresis of magnetite, *Earth planet. Sci. Lett.,* **169**(1-2), 51–58.

Muxworthy, A.R. & McClelland, E., 2000. Review of the low-temperature magnetic properties of magnetite from a rock magnetic perspective, *Geophys. J. Int.,* **140**(1), 101–114.

Nagasawa, Y., Kosaka, M., Katano, S., Môri, N., Todo, S. & Uwatoko, Y., 2007. Effect of uniaxial strain on Verwey transition in magnetite, *J. Phys. Soc. Jpn.,* **76**, 110–111.

Olivero, J.J. & Longbothum, R.L., 1977. Empirical fits to the Voigt line width: a brief review. *J. Quant. Spectrosc. Radiat. Transfer,* **17**(2), 233–236,

Pokorný, J., Suza, P. & Hrouda, F., 2004. Anisotropy of magnetic susceptibility of rocks measured in variable weak magnetic fields using the KLY-4S Kappabridge, *Geol. Soc. Spec. Publ.,* **238**, 69–76.

Ramasesha, S.K., Mohan, M., Singh, A.K., Honig, J.M. & Rao, C.N.R., 1994. High-pressure study of Fe3O4 through the Verwey transition, *Phys. Rev. B,* **50**(18), 13 789–13 791.

Reznik, B., Kontny, A., Fritz, J. & Gerhards, U., 2016. Shock-induced deformation phenomena in magnetite and their consequences on magnetic properties, *Geochem. Geophys. Geosyst.,* **17**(6), 2374–2393.

Rozenberg, G.K., Hearne, G.R., Pasternak, M.P., Metcalf, P.A. & Honig, J.M., 1996. Nature of the Verwey transition in magnetite (Fe3O4) to pressures of 16 GPa. *Phys. Rev. B,* **53**(10), 6482–6487.

Samara, G.A., 1968. Effect of pressure on the metal-nonmetal transition and conductivity of Fe3O4, *Phys. Rev. Lett.,* **21**(12), 795–797.

Sato, M., Yamamoto, Y., Nishioka, T., Kodama, K., Mochizuki, N. & Tsunakawa, H., 2012. Pressure effect on low-temperature remanence of multidomain magnetite: change in demagnetization temperature, *Geophys. Res. Lett.,* **39**(4), doi:10.1029/2011GL050402.

Senn, M.S., Loa, I., Wright, J.P. & Attfield, J.P., 2012. Electronic orders in the Verwey structure of magnetite, *Phys. Rev. B,* **85**(12), doi:10.1103/PhysRevB.85.125119.

Stoneham, A.M., 1969. Shapes of inhomogeneously broadened resonance lines in solids, *Rev. Mod. Phys.,* **41**(1), 82–108.

Succi, S. & Coveney, P.V., 2019. Big data: the end of the scientific method?, *Phil. Trans. R. Soc. A,* **377**(2142), doi:10.1098/rsta.2018.0145.

Syono, Y., 1965. Magnetocrystalline anisotropy and magnetostriction of Fe3O4-Fe2TiO4 series with special application to rocks magnetism, *Jpn. J. Geophys.,* **4**, 71–143.

Tamura, S., 1990. Pressure dependence of the verwey temperature of Fe3-yO4 obtained by Magnetic permeability measurements, *J. Phys. Soc. Jpn.,* **59**(12), 4462–4465.

Tong, X., Zhang, H. & Li, D.Y., 2015. Effect of annealing treatment on mechanical properties of nanocrystalline α-iron: an atomistic study, *Sci. Rep.,* **5**, doi:10.1038/srep08459.

Verwey, E.J.W., 1939. Electronic conduction of magnetite (Fe3O4) and its transition point at low temperatures, *Nature,* **144**, 327–328.

Walz, F., 2002. The Verwey transition—a topical review, *J. Phys. Condens. Matter,* **14**(12), R285–R340.

Whiting, E.E., 1968. An empirical approximation to the Voigt profile, *J. Quant. Spectrosc. Radiat. Transfer,* **8**(6), 1379–1384.

Wiecheć, A., Zach, R., Kąkol, Z., Tarnawski, Z., Kozłowski, A. & Honig, J.M., 2005. Magnetic susceptibility studies of single-crystalline zinc ferrites under pressure, *Physica B,* **359**, 1342–1344.

Williams, H.J., Bozorth, R.M. & Goertz, M., 1953. Mechanism of transition in magnetite at low temperatures, *Phys. Rev.,* **91**(5), 1107–1115.